Tracking using 3D Ultrasound for Guiding Cardiac Interventions

Bharat Ramachandran[a], Paul Thienphrapa[a,b], Ameet Jain[a] and Aleksandra Popovic[a]

[a]Philips Research North America, Briarcliff Manor, New York, NY 10510, USA.
[b]ERC CISST/LCSR, Johns Hopkins University, Baltimore, MD 21218, USA.

ABSTRACT

Cardiovascular disease is a leading cause of death in the United States with over 1 million people experiencing sudden cardiac death or myocardial infarction every year. There has been a growing interest in minimally invasive cardiac interventions and the global market for image guided navigation is estimated by some to grow to the tune of $600 million by 2015. 3D ultrasound is increasingly used by interventional cardiologists for procedures like device implantation, atrial septal defect and is often extended for providing therapy. In this work, we focus on tracking points on a biventricular phantom that mimics the motion of a beating heart in real-time using streaming trans-esophageal echocardiography (TEE) volumes. Accuracy is measured using simulations and manual verification. The result is that we are able to track points with mean RMS errors of 2.3mm. While the algorithm is run at 20Hz which is the update rate of TEE volumes in our system, the tracking can be performed at as high as 80Hz. Such real-time and robust tracking can be used for guiding cardiac interventions like targeted delivery of stem cells at the border of normal and infracted myocardial tissue. Alternately, in a military setting, we can use this scheme to track freely floating shrapnel within the chambers of the heart and perform retrieval of these fragments. We hope to repeat similar experiments in a pre-clinical setting to validate robustness of the algorithm and develop a flexible robotic system for performing the procedure minimally invasively.

Index Terms— Biventricular Phantom, Cardiac Interventions, Image-guided Navigation, TEE, Tracking

I. INTRODUCTION

Cardiovascular disease is the most common disease encountered in clinical practice today and is one of the leading causes of deaths in the United States [1]. The World Health Organization (WHO) projects cardiovascular diseases to cause over 23 million deaths per year worldwide by 2030 [2]. These cardiovascular diseases comprise of different disorders of the heart and blood vessels like coronary heart disease. Presently, over 19 million people around the world experience sudden cardiac death (SCD) or myocardial infarction (MI) every year [3]. When a portion of the lining of the coronary arteries that supply oxygen and nutrients to the myocardium develops atherosclerosis, the lining hardens and swells up to form a plaque. This obstructs the blood flow to the myocardium and causes coronary artery disease (CAD). Almost 80% of all SCD's are estimated to be a consequence of CAD [4]. If a plaque ruptures, blood is exposed to calcium and fatty deposits and forms clots which may partly or wholly block the artery and restrict the blood flow. The heart muscles being supplied by the occluded artery begin to die leading to MI and if a patient survives the acute MI, the resulting heart muscle damage may lead to chronic heart failure (CHF) or arrhythmias like atrial fibrillation (AF) or ventricular tachycardia (VT).

The treatment for these cardiac conditions has evolved over the past decade [5] and image-guided interventions are successfully replacing open heart surgery and other invasive surgical methods in many cases due to advantages like faster patient recovery time, lower risk of complications and lower cost. While many image-guided interventional procedures make use of pre-operative information of the anatomy using imaging techniques like magnetic resonance imaging (MRI) or computed tomography (CT) scans, these methods do not account for real-time intra-operative cardiac motion.

3D trans-esophageal echocardiography (TEE) can be used for near real-time interventional guidance during minimally invasive surgical procedures [6] since it offers, in addition to soft tissue contrast, volumetric imaging that enhances visualization of cardiac anatomy over B-mode ultrasound. Real-time tracking allows viewing of pre-selected points and creates a mechanism for intelligent and accurate interventions and therapy like drug delivery or stem cell injection.

The focus of this work is an algorithm which tracks in 3D, points on the surface of the heart in real-time using TEE volumes. The algorithm is optimized for a beating heart motion with large search volumes during the contraction and expansion phase of the heart cycle and smaller search volumes during the ventricular filling phase since this involves lesser motion. Tracking in TEE images is challenging due to the low signal to noise ratio (SNR), inherent speckle noise and limited field of view (FOV). The working of the algorithm is visualized using a graphic user interface (GUI), and is validated using simulated data undergoing translation and rotation and using in-vitro data from a biventricular phantom.

The long term objective of our project is to develop a flexible robotic system for minimally invasive retrieval of fragments from a beating heart under ultrasound guidance. We hope that this work on tracking the motion of *points on a beating heart* using sum of squared differences (SSD)—in conjunction with prior work on characterizing the motion of *fragments within a heart chamber* [7] using normalized cross-correlation (NCC)—can be used to analyze motion in the context of a robotic retrieval system in order to better understand the needs of and design and develop a robot control system capable of intelligent navigation and fragment retrieval.

II. METHODS

A. Background

3D TEE is a diagnostic tool for visualizing cardiac structures and diagnosing cardiovascular diseases. However, the presence of speckle noise and low SNR make fast and robust point tracking a challenging task; particularly feature tracking is harder in TEE volumes due to low SNR. The computational demand for tracking 3D TEE volumes is greater than 2D ultrasound images and due to the complex motion of the beating heart, a robust tracking algorithm should have the ability to detect error or drift and a mechanism for error correction. While the use of 3D TEE in tracking research is relatively new, several studies have explored other forms of 3D ultrasound [8]-[11]; however, the tracked targets have been limited to stationary objects. Motion of the mitral valve using 3D ultrasound has been demonstrated [12]-[13], though the tracking was performed via manual segmentation as opposed to the real-time tracking proposed here.

Many different techniques and tracking algorithms have been proposed in the past and one major class consists of maximum likelihood techniques that use accurate statistical models of the ultrasound images to estimate motion in B-mode images [14]. Another class of algorithms for motion estimation comprise of comparing intensity of image blocks [15]. Even though block matching schemes account for speckle pattern by representing it either as multiplicative Rayleigh noise or signal dependent additive Gaussian noise, such comparison of intensity of blocks using norms and tracking motion of pixels purely based on intensity have not been successful enough to apply in 3D tracking and are mostly used in 2D images. Automatic contour tracking [16] is a technique wherein the surface is treated as a parametric model with a sequential state space is used for tracking the contour of the left ventricle, but this has not been applied to tracking individual points. A set of points can be tracked by tracking the deformation state using a Kalman filter or predictor which is a recursive means to estimate the state of process while minimizing mean square error (MSE) and this supporting estimation of past present and future states [17]. An alternative to such a method could be to perform tracking by studying the motion of the heart, understanding the dynamic of the heart and specifically the left ventricle [18].

Another major class of tracking algorithms used for tracking in ultrasound images is based on sum square difference (SSD) and on correlation. Complex motions which can be modeled as a combination of translation, rotation and scaling can be tracked in the general framework of object tracking using SSD [19]. Real-time motion of internal organs can be tracked in 3D ultrasound images using SSD [20] since SSD based algorithms are efficient for registration with additive Gaussian nose and the logarithm performed to convert the radiofrequency data to B-mode images converts the multiplicative Raleigh noise to additive noise. SSD and cross-correlation coefficient (CC) along with maximum likelihood estimator (MLE) [21] have been applied to 3D cardiac ultrasound for applications such as atrial septal defect tracking [22]. All aforementioned techniques apply universal description of objects without considering any temporal relationships, which leads to temporal inconsistence between adjacent frames.

To overcome this difficulty, one step forward prediction [23] using motion manifold learning which estimates posterior probability using past measurements and a recursive process having a prediction step and an updating step can be used for fast and accurate tracking of the left ventricle [24]. Other techniques such as tracking deforming objects using particle filtering [25], fast point tracking algorithm [26], demon's algorithm [27] and condensation algorithm [28] have been suggested.

Fig. 1. Experimental setup showing the dynamic heart phantom in a water tank, a TEE probe secured within a probe holder and an ultrasound machine showing the phantom volume using a live 3D visualization scheme.

B. Experimental Setup

The experimental setup shown in Fig. 1 consists of a beating heart phantom kept within a water tank, an ultrasound machine and a workstation (2.3 GHz Intel Xeon, 4 GB of RAM) that acquires live streaming ultrasound volumes over TCP/IP.

The phantom is a custom developed biventricular multi-modality beating heart phantom [29] which is visible under X-ray, ultrasound and magnetic resonance imaging (MRI). It is made of polyvinyl alcohol cryogen (PVA), is a replica of the human heart and is kept within an acrylic glass water tank. Water is pumped into and out of the phantom using two servo-actuated pneumatic pistons that create the deformable effect of heart beat and blood flow. A heart rate of 1 Hz and stroke volume lower than in healthy humans were chosen in the experiments in order to mimic surgical [30] and post-injury cardiovascular conditions.

The Philips iE33 xMATRIX Echocardiography System is used with the X7-2t 2D TEE probe. Each image has a resolution of 128x48x112 voxels of size 0.81, 0.96, and 0.98 mm, spanning a field of view of 60° azimuth, 30° elevation and 12 cm depth respectively. Gain is set at 47% and compression at 40 dB.

C. SSD based Tracking Algorithm

SSD is a standard technique to measure similarity and is one of the choices for tracking myocardial motion using 3D ultrasound. Due to its real-time, efficient and robust performance while tracking points in noisy ultrasound images, coupled with the fact that this scheme can be easily extended to track a fragment within the chamber that is visible in live TEE images, we chose SSD as the principle for our tracking algorithm.

The formula for calculating the SSD metric is given in (1) where f is the 3 dimensional image, g is the template and summation is over the positions x, y, z under the template positioned at u, v, w. In other words, f is the reference image or mask and g is the search region, both in three dimensions, and d^2 is the distance which needs to be minimized.

$$d^2(u,v,w) = \sum_{x,y,z} [f(x,y,z) - g(x-u, y-v, z-w)]^2 \quad (1)$$

We define a weighted squared difference *(WSD)* that is used for similarity matching and is defined as given in (2) where k is a weight/ integer equaling the number of elements in the mask.

$$WSD = ArgMin[d^2 / k] \quad (2)$$

The squared difference divided by the weight is minimized and a *WSD* value is obtained. This measure is used to calculate similarity and predict the motion undergone by the point of interest, thereby tracking the selected point on the TEE image.

Apart from the point to be tracked after manual selection, the mask size and search space are defined by the user. Similarity matching is performed and if the match is bad, then the error is detected and another match is performed over a larger search space. Despite this, if the error is high, then a comparison is performed between the mask from the initial frame and the current frame. Once the optimized squared difference gives the distance by which the point has moved, this new frame is set as the reference frame and compared to the next incoming frame. A flowchart describing the different steps of the SSD based tracking algorithm is shown in Fig. 2.

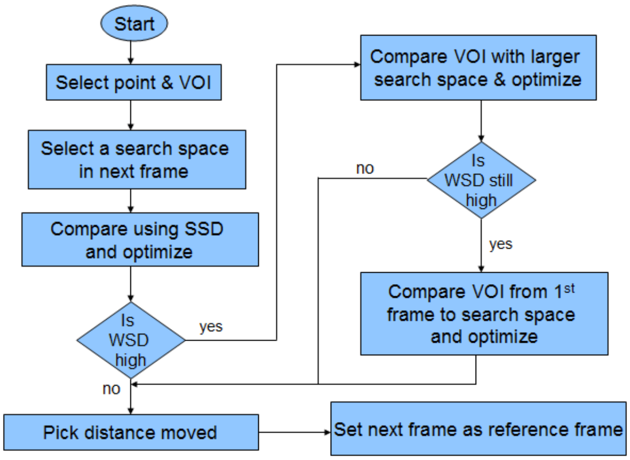

Fig. 2. Flowchart showing the working of the SSD based tracking algorithm.

D. Simulation of Data

In order to verify and validate the working of the point tracking algorithm and to determine its speed and accuracy, the tracking algorithm was run on simulated data. The simulation consisted of rotation, translation and scaling performed to different extents, wherein to and fro rotation about the Z-axis and to and fro translation in the X and Y direction mimicked the motion of the myocardium. The transformation matrix M is a 4 by 4 matrix that produces the net effect of rotation, translation and scaling along every direction. To ensure consistency while performing simulations, 3D TEE volumes at end diastole were taken as the reference. The flowchart in Fig. 3 explains the method to perform simulations.

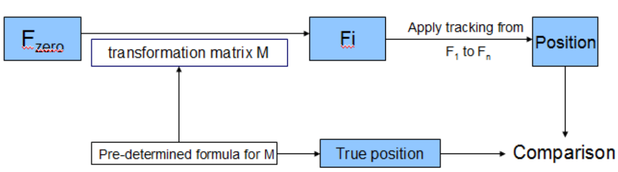

Fig. 3. Flowchart showing simulation to validate the algorithm.

The reference image shown as F_{zero} is taken at the end diastole phase of the cardiac cycle and the transformation matrix M is applied to it. The values of M are pre-determined by formula determining the extent of rotation, translation and scaling as input by the user. The tracking algorithm is applied to the different simulated images shown as F_i in the flowchart. The output given by the tracking algorithm is compared with the true position that is known from the pre-determined formula. This method is followed to predict the accuracy and robustness of the tracking algorithm, and verify and validate its working under different conditions of rotation, translation and scaling undergoing motions similar to that of the myocardium.

E. GUI for Tracking

To track a point over time, it is necessary to select the point on the 3D TEE image and view it and its features first. A basic GUI was built using Matlab (The Mathworks Inc.,) platform. This GUI shows the three perpendicular views, namely axial, coronal and sagittal, of the ultrasound image at one time frame. The user has the ability to select any point by clicking on any of the three views. The current selected point is shown by the point of intersection of two perpendicular blue lines and its coordinates and value are displayed on the lower right display. When the user wants to define a region of interest (ROI) around the area to be tracked, he/she can define the features of the ROI in terms of its dimensions and angulations. The user then has the ability to perform tracking from live 3D TEE volumes. Alternately, the user can save a volume, load it and perform tracking on the same. The user may also choose to stream the TEE volumes without tracking in order to position the probe. A screenshot of the GUI is shown in Fig. 4.

III. RESULTS

The algorithm was tested on both simulated and real-time phantom 3D TEE data. Quantitative results were obtained from the simulated datasets which helped determine the speed, accuracy and robustness of the algorithm, while qualitative results were obtained from the phantom datasets which helped visualize the tracking over time.

To obtain the results from the simulated datasets that were closest to the real heart motion, the parameters of the transformation matrix were chosen to mimic the myocardial motion i.e. to and fro rotation about the Z axis and to and fro translation along the X and Y directions. The mask size of 3x3x3 pixels was chosen and the default search space was set as 5x5x5 pixels. The WSD value was detected and compared and if it was high, a larger search space was chosen and the matching was performed again. The plot in Fig. 5 shows absolute error in pixels plotted against the frame number for 3 different cases, namely fixed search space with no error detection, and correction with search space of 7x7x7 and 9x9x9. It is seen that when the search space is fixed at 5x5x5 the error is high. Increasing the search space by comparing the WSD value used for detecting the loss of a feature such as ventricular contraction reduces the error. This technique of increasing the search space based on the WSD value results in an inherent advantage over setting a larger search space as default since it improves the computational time involved.

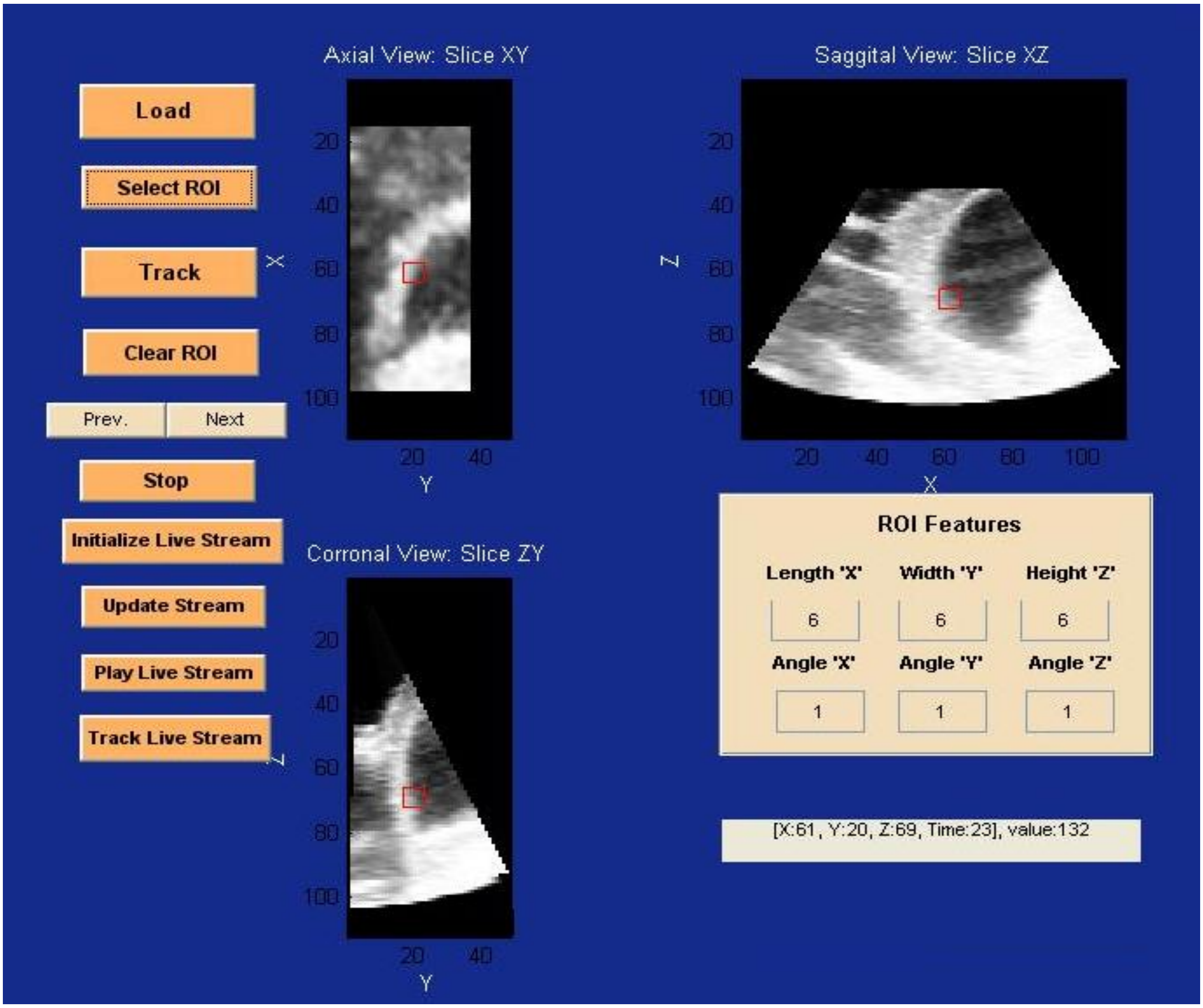

Fig. 4. Snapshot of the GUI showing the orthogonal slices of a 3D TEE volume of the heart phantom. The red square that corresponds to the feature of interest can be defined by the user to either track a point on the surface or boundary of the myocardium or a fragment within the chambers of the heart.

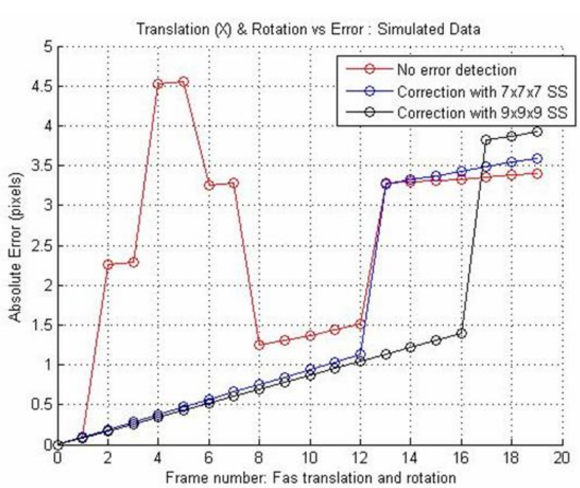

Fig. 5. Plot of absolute error in pixels against frame number in case of simulation mimicking cardiac motion without and with error correction.

However, while the frame number increases, the absolute error also increases gradually. Also, the mean RMS error over 10 simulated datasets was found to be 2.3 mm after 20 frames.

Next, the results of the speed of the algorithm were determined using similar simulated datasets. Even in this case, parameters of the transformation matrix were chosen to simulate cardiac motion. The run-time for a single iteration for different search space and mask size as well as the case with correction is plotted in Fig. 6.

For a fixed mask size, the run-time increases with increase in search space. A mask size of 3x3x3 pixels takes only 0.01 seconds with a search space of 5x5x5 pixels but takes 0.042 seconds when the neighborhood is increased to 9x9x9 pixels.

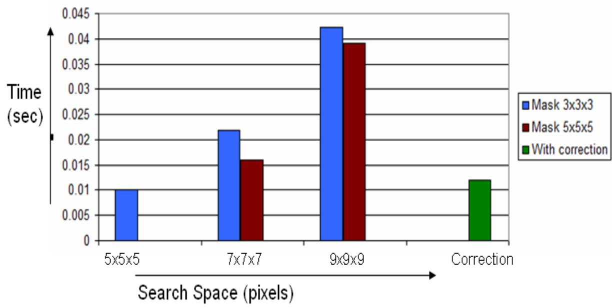

Fig. 6. Plot of run-time against different search space and mask combinations and run-time for the case with correction.

The result also shows that for a fixed search space, a larger mask takes lower time as compared with a smaller mask. We observe that the time increases with an increase in search space and mask size. In the case of with correction, the default mask is set as 3x3x3 pixels and the default search space as 5x5x5 pixels. In case of loss of feature, the search space increases to 9x9x9 pixels, and despite this, if the WSD is high, a comparison is performed with the first frame, with the mask as 3x3x3 pixels in the initial frame and a search space of 9x9x9 pixels. The run-time with such correction is 0.012 seconds on an average, thus, we achieve the accuracy of a larger search space and mask at speeds close to 80 Hz that are obtained by a smaller mask and search space.

IV. CONCLUSION & FUTURE WORK

An algorithm for tracking points in live 3D TEE volumes in order to guide cardiac interventions is presented. We conclude that the tracking was accurate, real-time and robust for our clinical problem. The detection of drift using WSD and its correction significantly improved the robustness of the algorithm. However, the spatial and temporal resolution of the data significantly influenced the performance of the algorithm. This understanding will be critical in improving the robustness of tracking during future clinical interventions. As future work, an ECG/state-space based correction needs to be incorporated that additionally performs a similarity measure at every end diastole. Finally, these preliminary results show promise towards improving the robustness of motion tracking in low resolution volume streams as well as extending this work to achieve our long term objective of tracking the heart and fragments within it simultaneously in order to perform an ultrasound guided minimally invasive robotic intervention for retrieval of fragments and shrapnel from within the heart.

ACKNOWLEDGEMENT

The authors would like to thank Douglas Stanton, Haytham Elhawary and Vijay Parthasarathy, all from Philips Research North America for their contributions, help and invaluable feedback.

REFERENCES

[1] Arialdi M. Miniño, Elizabeth Arias, Kenneth D. Kochanek, Sherry L. Murphy, Betty L. Smith. Deaths: Final Data for 2000. National vital statistics reports; vol 50, no 15. Hyattsville, MD: National Center for Health Statistics. 2002.

[2] http://www.who.int/mediacentre/factsheets/fs317/en/index.html

[3] S. Yusuf, S. Reddy, S. Ounpuu, S. Anand, "Global burden of cardiovascular diseases: part I; general considerations, the epidemiologic transition, risk factors, and impact of urbanization," Circulation 104(22) (2001) 2746-2753.

[4] D. Zipes, J. Jalife, "Cardiac electrophysiology: from cell to bedside," 4th edn. W B Saunderscompany, Philadelphia, PA. (2004).

[5] Z. Malchano, "Image guidance in cardiac electrophysiology," Master's thesis, Massachusetts Institute of Technology, Boston, MA (June 2006).

[6] C. Hammerstringl, L. Lickfett, G. Nickeneg, "Real-time three dimensional transoesophageal echocardiography for guidance of interventional closure of paravalvular leakage," European Heart Journal 2009 30(8):915.

[7] P. Theinphrapa, H. Elhawary, B. Ramachandran, D. Stanton, A. Popovic, "Tracking and characterization of fragments in a beating heart using 3D ultrasound for interventional guidance . MICCAI 2011, LNCS 6891, pp. 211 – 218, 2011.

[8] J. A. Stoll, P. M. Novotny, R. D. Howe, and P. E. Dupont, "Real-time 3D ultrasound-based servoing of a surgical instrument," in IEEE Int. Conf. on Robotics and Automation, pp. 613-618.

[9] P. M. Novotny, J. A. Stoll, P. E. Dupont, and R. D. Howe, "Real-time visual servoing of a robot using three-dimensional ultrasound," in IEEE Int. Conf. on Robotics and Automation, pp. 2655-2660.

[10] J. Whitman, M. P. Fronheiser, and S. W. Smith, "3-D ultrasound guidance of surgical robotics using catheter transducers: feasibility study," IEEE Trans.Ultrason., Ferroelectr., vol. 55, pp. 1143-1145, 2008.

[11] K. Liang, D. V. Allmen, A. J. Rogers, E. D. Light, and S. W. Smith, "Three-dimensional ultrasound guidance of autonomous robotic breast biopsy: feasibility study," vol. 36, pp. 173-177, 2010.

[12] S. G. Yuen, D. T. Kettler, P. M. Novotny, R. D. Plowes, and R. D. Howe, "Robotic motion compensation for beating heart intracardiac surgery," vol. 28, pp. 1355-1372, 2009.

[13] S. B. Kesner, S. G. Yuen, and R. D. Howe, "Ultrasound servoing of catheters for beating heart valve repair," in Int. Conf. on Info. Proc. in Computer-Assisted Interventions, Berlin, Heidelberg, pp. 168-178.

[14] M. F. Insana, L. T. Cook, M. Bilgen, P. Chaturvedi, Y. Zhu, "Maximum-likelihood approach to strain imaging using ultrasound," The Journal of the Acoustical Society of America, 2000.

[15] M. G.Strintzis, I. Kokkinidis, "Maximum Likelihood Motion Estimation in Ultrasound Image Sequences," IEEE Signal Processing Letters, 1997 4(6).

[16] M. Li, C. Kambhamettu, M. Stone, "Automatic Contour Tracking in Ultrasound Images," Clinical linguistics & phonetics, 2005.

[17] F. Orderud, "A Framework for real-time left ventricular tracking in 3D+T echocardiography, using nonlinear deformable contours and kalman filter based tracking," Computers in Cardiology, pages 125-128, 2006.

[18] S. Malassiotis, M. G. Strintzis, "Tracking the left ventricle in echocardiographic images by learning heart dynamics," IEEE transactions on medical imaging, 1999.

[19] G. D. Hager, P. N. Belhumeur, "Efficient region tracking with parametric models of geometry and illumination," Pattern Analysis and Machine Intelligence, 1998.

[20] S. Xu, S. Settlemeir, B. J. Wood, “Real-time motion tracking using 3D ultrsound,” Medical Imaging 2007.

[21] B. Cohen, I. Dinstein, “New maximum likelihood motion estimation schemes for noisy ultrasound images,” Pattern Recognition, Vol. 35 (2002) 455-463.

[22] M. G. Linguraru, N. V. Vasilyev, P. J. del Nido, R. D. Howe, “Atrial Septal defect tracking in 3D cardiac ultrasound,” MICCAI 2006, LNCS 4190, pp. 596 – 603, 2006.

[23] L. Yang, B. Georgescu, Y. Zheng, P. Meer, D. Comaniciu, “3D ultrasound tracking of the left ventricle using one-step forward prediction and data fusion of Collaborative Trackers,” IEEE Conference on Computer Vision and Pattern Recognition, 2008.

[24] L. Yang, B. Georgescifi, Y. Zheng, D. J. Foran, D. Comaniciu, “A fast and accurate tracking algorithm of left ventricles in 3D echocardiography,” 5th IEEE International Symposium on Biomedical Imaging, 2008.

[25] Y. Rathi, N. Vaswani, A. Tannenbaum, A. Yezzi, “Tracking deforming objects using particle filtering for geometric active contours,” IEEE transactions on pattern analysis and machine intelligence 2007.

[26] C. J. Veenman, E. A. Hendriks, M. J. T. Reinders, “A fast and robust point tracking algorithm,” Image Processing, 1998.

[27] X. Pennec, P. Cachier, N. Ayache, “Understanding the " demon's algorithm": 3D non-rigid registration by gradient descent,” Lecture Notes in Computer Science, 1999.

[28] E. B. Koller-Meier, F. Ade, “Tracking multiple objects using the condensation algorithm,” Robotics and Autonomous Systems, 2001.

[29] Shelley Medical Imaging Technologies: Multi-modality Dynamic Heart Phantoms, http://www.simutec.com/dynamic_hearts.html.

[30] K. L. Ryan, W.H. Cooke, C.A. Rickards, K.G. Lurie, V.A. Convertino, “Breathing through an inspiratory threshold device improves stroke volume during central hypovolemia in humans,” J. Appl. Physiol. 104(5), 1402-9 (2008).